

100★

Basic and Clinical Thoracic Surgery 2

Editör

Aykut ELİÇORA



BIDGE Publications

Basic and Clinical Thoracic Surgery 2

Editor: Doç. Dr. Aykut Eliçora

ISBN: 978-625-372-541-9

Page Layout: Gözde YÜCEL

1st Edition:

Publication Date: 25.12.2024

BIDGE Publications,

All rights of this work are reserved. It cannot be reproduced in any way without the written permission of the publisher and editor, except for short excerpts to be made for promotion by citing the source.

Certificate No: 71374

Copyright © BIDGE Publications

www.bidgeyayinlari.com.tr - bidgeyayinlari@gmail.com

Krc Bilişim Ticaret ve Organizasyon Ltd. Şti.

Güzeltepe Mahallesi Abidin Daver Sokak Sefer Apartmanı No: 7/9 Çankaya /
Ankara



Content

Comparison of Skeletonized and Pedicled Harvesting Techniques of the Internal Mammarian Artery in Terms of Postoperative Hemorrhage.....	4
Alper ERKİN.....	4
M. Kaan KIRALI	4
Early detection of cardiovascular disease using deep learning technique	28
Harun SELVİTOPI	28
Seda DEMİR	28
Mesothelioma.....	37
Aykut ELİÇORA.....	37
Carcinoid Tumor: A Rare Primary Bone Localization? Bone Metastasis?	51
Mertay Boran.....	51
Mohammed Jebeli	51
Reşad Kızılok	51
Asuman Kilitçi	51

CHAPTER I

Comparison of Skeletonized and Pedicled Harvesting Techniques of the Internal Mammarian Artery in Terms of Postoperative Hemorrhage

Alper ERKİN¹
M. Kaan KIRALI²

Introduction

The use of the internal mammary artery (IMA) in coronary artery bypass surgery (CABS) remains the gold standard. The internal mammary artery has a dense and non-penetrated intact elastic lamina and a thin media layer containing few smooth muscle cells. With this structure, the IMA resists intimal hyperplasia and medial calcification through inhibition of cellular migration,

¹ Assist. Prof. Dr., Sakarya University, Sakarya Faculty of Medicine, Cardiovascular Surgery Department, Sakarya/Turkey, Orcid: 0000-0001-6144-3727, alperkin@hotmail.com

² Prof. Dr., SBU, Kartal Koşuyolu Yüksek İhtisas Training and Research Hospital, Cardiovascular Surgery Department, Istanbul/Turkey, Orcid: 0000-0003-0044-4691, imkbkirali@yahoo.com

resulting in longer patency rates. The internal mammary artery is removed by two techniques: pedicled and skeletonized technique (Henriquez-Pino et al., 1997; www.medicine.ankara.edu.tr/surgical_type/kvc/modules; De Jesus & Acland 1995).

Skeletonization is a special technique that separates the IMA from its surrounding tissues, allowing meticulous removal without damaging the internal thoracic vein and collateral blood supply of the sternum. IMAs harvested using the skeletonized technique have a longer graft length. The longer graft length prevents tension that may develop due to lung expansion and prevents complications that may develop due to short graft length, especially in people with chronic obstructive pulmonary disease (Pevni et al., 2003; Tatoulis, Buxton & Fuller 1997).

At the same time, the long graft prepared with the skeletonized technique increases the number of vessels revascularized with arterial graft by allowing anastomosis to multiple vessels with consecutive technique. Since the skeletonization technique does not damage the sternal collateral circulation, it provides better blood supply to the sternum in the postoperative period. Therefore, patients who undergo IMA removal with the skeletonized technique have fewer sternal wound infections in the postoperative period (Arnold, 1972; Seyfer et al., 1988). Patients with skeletonized IMA removal show less need for blood transfusion and shorter intensive care unit and hospital stays in the postoperative period (Peterson et al., 2003; Calafiore et al., 1999). The aim of this study was to compare the effect of skeletonized and pedicled techniques for IMA release on early outcomes, especially on postoperative bleeding and blood transfusion.

Material and Method

Patient Group

In this study, we prospectively evaluated the early postoperative results of 217 patients, 177 (81.56%) males and 40 (18.44%) females, who underwent coronary artery bypass surgery using IMA graft between June 25, 2010 and September 30, 2010 in the Cardiovascular Surgery Clinic of Kartal Kosuyolu High Specialization Training and Research Hospital. Patients who underwent endarterectomy of the coronary arteries and combined coronary artery surgery were excluded from the study. Preoperative, perioperative and early postoperative data of the patients were obtained by a detailed examination of the files kept in the archives of our hospital. Two different techniques were applied during IMA release in the patients included in the study and the patients were divided into 2 groups. Group P consisted of 163 patients (75.11%) who underwent CABC operation using pedicled IMA and Group S consisted of 54 patients (24.89%) who underwent CABC operation using skeletonized IMA. The operation was planned for all patients according to the decision of the Cardiology-Cardiovascular Surgery joint council of our hospital.

Surgical Technique

After preoperative preparations, the patients underwent median sternotomy under standard anesthesia technique. The IMA graft was then prepared with two techniques.

Skeletonized Technique

After median sternotomy, an IMA retractor was placed to provide optimal visualization. The internal mammary artery was gently freed with the tip of the cautery, leaving the associated veins,

fascia and adipose tissue in place. The incision in the endothoracic fascia was started distally at the level of the sixth intercostal space. Side branches were cut using the double clip technique. If the length of the side branch did not allow two clips to be placed safely, one clip was placed on the IMA side and then the side branch on the wall side was cut by licking the wall with cautery. After making sure that the side branches were completely clipped and transected, the small amount of surrounding tissue adherent to the IMA was separated using low cautery or coronary scissors. After the distal part of the internal mammary artery was dissected, the endothoracic fascia was cut proximally with cautery. When the most proximal part of the internal mammary artery was reached, the pericardial branches were clipped. The IMA was then evaluated for inadequate hemostasis and trauma. Foci of bleeding were controlled by clipping or suturing. Heparin was administered before transecting the distal part of the internal mammary artery. Hemostasis was achieved by clipping the distal IMA fragment remaining in the wall, leaving the bifurcation area intact. The IMA was then placed in diluted papaverine gas.

Pedicle Technique

After sternotomy, optimal visualization was achieved with an IMA retractor. The endothoracic fascia was incised at the level of the bifurcation at the sixth intercostal space and then extended to the first intercostal space. Retraction of the pedicle allowed exposure of the communicating veins and the IMA itself. The perforator and anterior intercostal branches were cut using the double clip technique if their length was sufficient. If the lateral branches were short, they were clipped in such a way that they did not cause narrowing of the IMA lumen and were cut close to the chest wall with an electrocautery. The distal IMA was ligated with 3/0 dextron

suture material and clipped once, and then the IMA was cut just anterior to the bifurcation. The removed IMA was placed in diluted papaverine gas.

Statistics

In statistical evaluation, data analyses were performed using the SPSS program. Parametric data were calculated as mean and standard deviation and categorical data were calculated as percentage. Parametric data with normal distribution were evaluated using unpaired t test, categorical data with normal distribution were evaluated using chi-square test and Fisher's exact test if appropriate. Pearson correlation test was used to evaluate the relationship between parametric data. Results were considered significant when the p value was less than 0.05 in intergroup comparisons.

Findings

The data of the patients included in the study were grouped as preoperative, perioperative and postoperative data.

Preoperative Data

When the preoperative data of the patients in Group P and Group S were compared, no statistically significant difference was found in general (Table 1). Only the mean weight of the patients in Group S was found to be statistically significantly higher ($p = 0.026$).

Table 1: Preoperative data

	Group P	Group S	<i>p</i>
Age (years)	59.09 ± 10.51	59.06 ± 10.18	0.982
Height (cm)	163.17 ± 8.72	165.63 ± 9.04	0.077
Weight (kg)	75.64 ± 13.68	80.22 ± 10.78	0.026
Gender (male)	131 (%80.4)	46 (%85.2)	0.429
EuroSCORE	3.72 ± 3.91	3.59 ± 3.31	0.830
USAP	57 (%35.0)	25 (%46.3)	0.137
Family History	64 (%39.39)	20 (%37.0)	0.771
Previous MI	88 (%54.0)	27 (%50.0)	0.611
Cigarette	96 (%58.9)	30 (%56.6)	0.769
Hypertension	90 (%55.2)	36 (%66.7)	0.139
DM	54 (%33.1)	19 (%35.2)	0.782
COPD	24 (%14.7)	8 (%14.8)	0.987
Dyslipidemia	106 (%65.0)	41 (%75.9)	0.138
KBY	12 (%7.4)	5 (%9.3)	0.653
Non-cardiac arteriopathy	15 (%9.2)	7 (%13.0)	0.427

DM: diabetes mellitus, **CRF:** chronic renal failure, **MI:** myocardial infarction, **USAP:** unstable angina pectoris

The mean weight of the patients in group P was 75.64 ± 13.68 kg and that of the patients in group S was 80.22 ± 10.78 kg. The mean weight of the patients in group S was statistically significantly higher (Figure 1).

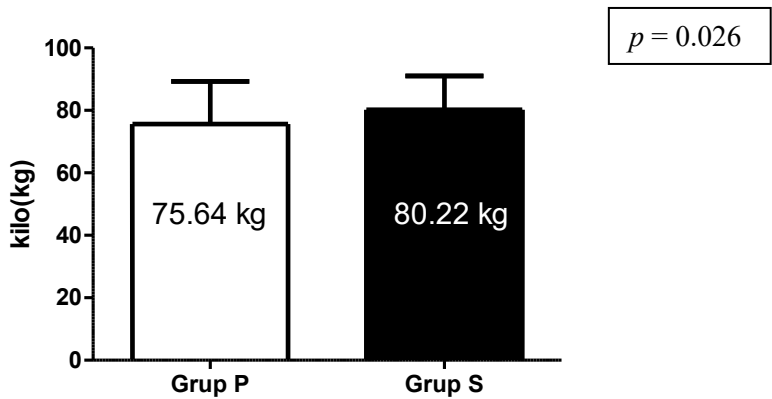


Figure 1: Mean weight of Group P and Group S

Perioperative Data

When patients in group P and group S were compared in terms of preoperative heparin use, no statistically significant difference was found (Table 2).

Table 2: Comparison of the groups in terms of preoperative heparin use

		preop heparin (-)	preop heparin (+)	Total	<i>p</i>
	N	95	68	163	
Group P	group %	%58.30	%41.70	%100	
	Total %	%43.80	%31.30	%75.10	0.899
	N	32	22	54	
Group S	group %	%59.30	%40.70	%100	
	Total %	%14.70	%10.20	%24.90	

preop: Before surgery

When patients in group P and group S were evaluated in terms of whether the operation was performed in beating heart or perfusion, no statistically significant difference was found (Table 3).

Table 3: Comparison of groups in terms of operation on beating heart and operation under cardiopulmonary bypass

		KPB	BH	Total	<i>p</i>
	N	133	30	163	
Group P	group %	%81.60	%18.40	%100	
	Total %	%61.30	%13.80	%75.10	0.773
	N	45	9	54	
Group S	group %	%83.30	%16.70	%100	
	Total %	%20.70	%4.20	%24.90	

BH: Working heart, **CPB:** Cardiopulmonary bypass

There was no statistically significant correlation between the number of distal anastomoses performed and the amount of postoperative drainage in patients in group P and group S according to whether the operation was performed in perfusion or beating heart (Table 4).

Table 4: Evaluation of the groups in terms of the correlation of the number of anastomoses with postoperative drainages

				po (0) drainage	po (1) drainage	po (2) drainage	Total drainage
		anasto mosis	pearson correlation	0.114	0.029	0.076	0.105
	K PB	Numbe r of	<i>p</i>	0.193	0.737	0.384	0.228
Grou p P			N	133	133	133	133
		anasto mosis	pearson correlation	-0.034	-0.060	0.150	0.061
	B H	Numbe r of	<i>p</i>	0.857	0.752	0.430	0.750
			N	30	30	30	30
		anasto mosis	pearson correlation	-0.008	0.109	0.096	0.048
	K PB	Numbe r of	<i>p</i>	0.959	0.477	0.530	0.754
Grou p S			N	45	45	45	45
		anasto mosis	pearson correlation	0.063	-0.390	-0.278	-0.125
	B H	Numbe r of	<i>p</i>	0.871	0.299	0.454	0.749
			N	9	9	9	9

BH: Working heart, **CPB:** Cardiopulmonary bypass, **po:** Postoperative

There was no statistically significant correlation between the end-of-case ACT value and the day of surgery and total drainage in patients in group P and group S according to whether the operation was performed in perfusion or beating heart (Table 5).

Table 5: Evaluation of the groups in terms of correlation of end-of-case ACT values with postoperative drainages

				po (0) drainage	Total drainage
		end of case	pearson correlation	0.072	0.053
	KP B	ACT	p	0.413	0.548
Group P			N	133	133
		end of case	pearson correlation	0.207	0.145
	BH	ACT	p	0.271	0.446
			N	30	30
		end of case	pearson correlation	0.246	0.164
	KP B	ACT	p	0.104	0.282
Group S			N	45	45
		end of case	pearson correlation	-0.230	-0.344
	BH	ACT	p	0.552	0.365
			N	9	9

BH: Working heart, **CPB:** Cardiopulmonary bypass, **po:** Postoperative

When patients in group P and group S were compared in terms of protamine use, no statistically significant difference was found (Table 6).

Table 6: Comparison of the groups in terms of protamine use

		protamine (-)	protamine (+)	Total	<i>p</i>
	N	101	62	163	
Group P	group %	%62.00	%38.00	%100	
	Total %	%46.50	%28.60	%75.10	0.896
	N	34	20	54	
Group S	group %	%63.00	%37.00	%100	
	Total %	%15.70	%9.20	%24.90	

Patients in group P and group S were compared in terms of transamine use and no statistically significant difference was found between the groups in terms of transamine use (Table 7).

Table 7: Comparison of the groups in terms of transamine use

		transamine (-)	transamin (+)	Total	<i>p</i>
	N	140	23	163	
Group P	group %	%85.90	%14.10	%100	
	Total %	%64.50	%10.60	%75.10	0.575
	N	48	6	54	
Group S	group%	%88.90	%11.10	%100	
	Total %	%22.10	%2.80	%24.90	

Group P and group S were compared in terms of postoperative heparin use. It was observed that 8% of patients in the pedicled IMA removal group and 20.4% of patients in the skeletonized IMA removal group used heparin in the postoperative period (Figure 2). Our results showed a statistically significant higher rate of heparin use in the postoperative period in the skeletonized group (Table 8).

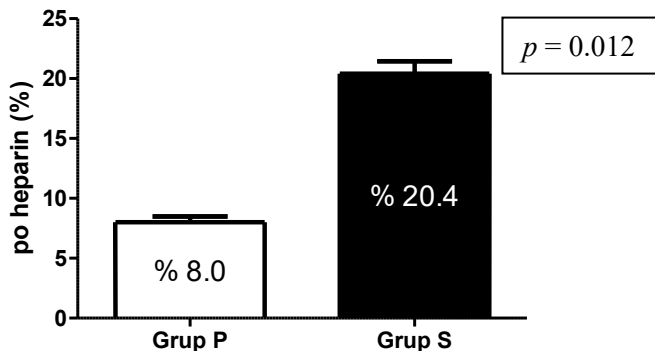


Figure 2: Comparison of postoperative heparin use

Table 8: Comparison of the groups in terms of postoperative heparin use

		po heparin (-)	po heparin (+)	Total	<i>p</i>
	N	150	13	163	
Group P	group %	%92.00	%8.00	%100	
	Total %	%69.10	%6.00	%75.10	0.012
	N	43	11	54	
Group S	group %	%79.60	%20.40	%100	
	Total %	%19.80	%5.10	%24.90	

po: Postoperative

There was a positive correlation between the presence or absence of plaque in the LAD and postoperative heparin use in patients in group P and group S (Table 9).

Table 9: Correlation of left anterior descending artery vessel quality with postoperative heparin use

			po heparin
	pearson correlation		0.200
Group P	<i>p</i>	LAD plaque	*0.010
	N/n		163 /40
	pearson correlation		0.325
Group S	<i>p</i>	LAD plaque	*0.016
	N/n		54 /18

*Correlation is significant at $p < 0.05$. **po:** Postoperative

Postoperative Data

Postoperative Bleeding and Blood Product Transfusion

Although there was no statistically significant difference in terms of drainage on the day of surgery, first and second postoperative day drainage and total drainage were statistically significantly less in Group S. Similarly, blood transfusion was also less in the group with skeletonized IMA removal (Table 10).

Table 10: Postoperative drainage amounts and blood transfusion requirement

	Group P	Group S	<i>p</i>
po (0) drainage (mL)	652.76 ± 296.82	688.89 ± 315.73	0.409
po (0) drainage (mL/kg)	9.35 ± 7.80	8.80 ± 4.63	0.627
po (1) drainage (mL)	303.68 ± 203.71	129.63 ± 129.77	< 0.001
po (2) drainage (mL)	91.72 ± 193.98	22.22 ± 67.76	0.011
Total drainage (mL)	1064.72 ± 537.88	850.00 ± 382.77	0.007
Blood transfusion (U)	2.88 ± 2.29	1.50 ± 1.24	< 0.001

po: Postoperative

There is a statistically highly significant difference between group P and group S in terms of drainage on postoperative day 1 (Figure 3).

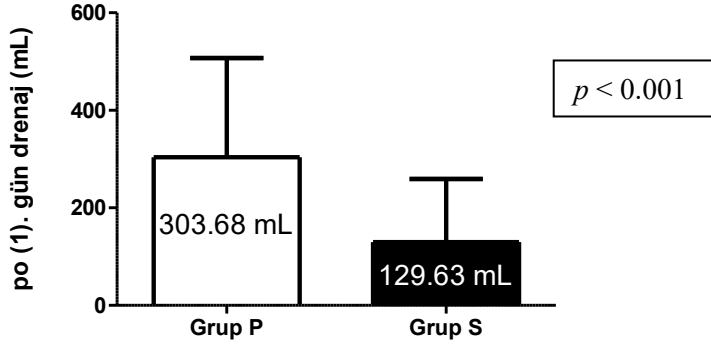


Figure 3: Comparison of the amount of drainage on the first postoperative day

There is a statistically significant difference between group P and group S in terms of drainage on postoperative day 2 (Figure 4).

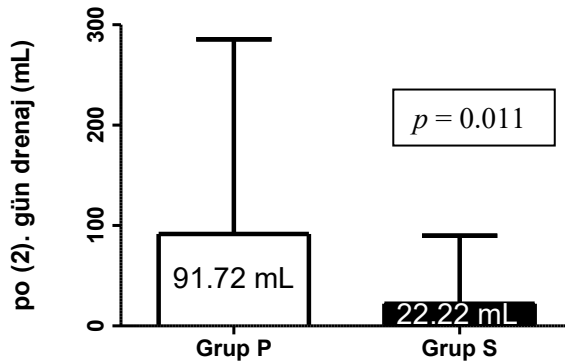


Figure 4: Comparison of the amount of drainage on the second postoperative day

There is a statistically significant difference between group P and group S in terms of total drainage amount (Figure 5).

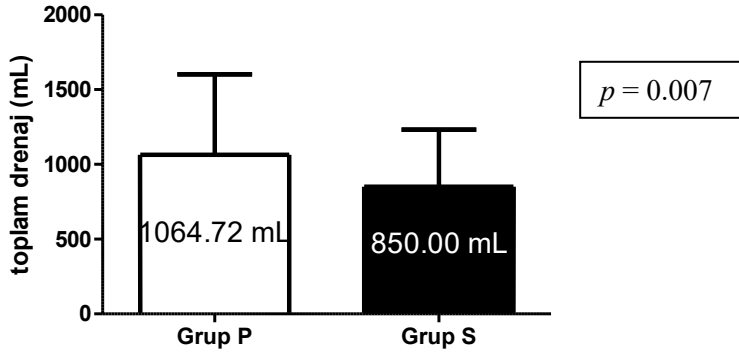


Figure 5: Comparison of the total amount of drainage

There was a highly statistically significant difference between group P and group S in terms of postoperative blood transfusion (Figure 6).

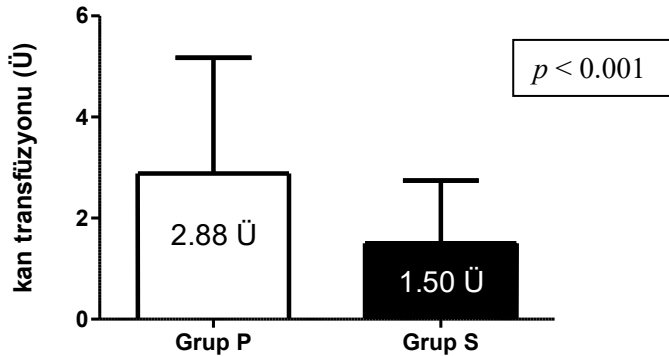


Figure 6: Comparison of transfusion requirement

Early Morbidity

Early postoperative data of patients in Group P and Group S were compared (Table 11).

Table 11: Evaluation of postoperative data

	Group P	Group S	<i>p</i>
Revision	8 (%4.9)	1 (%1.9)	0.329
Deep sternal infection	9 (%5.6)	0 (%0)	0.077
Superficial sternal infection	29 (%17.9)	3 (%5.6)	0.027
Mortality	9 (%5.5)	1 (%1.9)	0.265
po tamponad	2 (%1.2)	0 (%0)	0.413
Duration of ICU stay (days)	3.99 ± 5.07	1.98 ± 2.12	0.005
Length of hospital stay (days)	9.72 ± 6.30	6.57 ± 2.37	< 0.001

po: Postoperative, ICU: Intensive care unit

There was no statistically significant difference in deep sternal wound infection between patients with pedicled IMA removal and patients with skeletonized IMA removal. There was a statistically significant higher rate of superficial sternal wound infection in the pedicled IMA removal group (Figure 7).

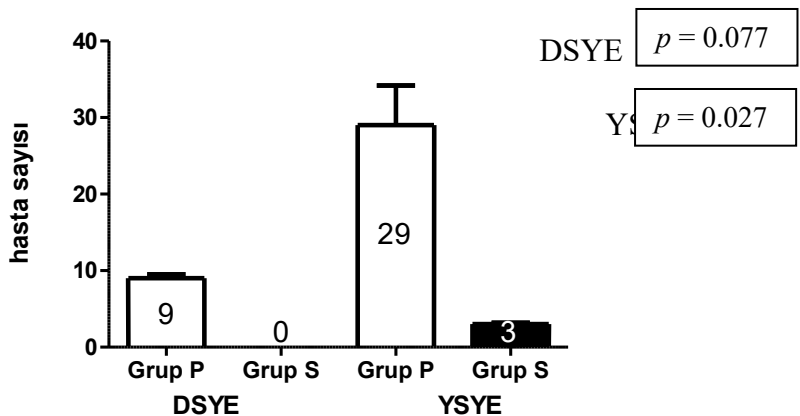


Figure 7: Postoperative. comparison of cases with deep and superficial sternal infection

***DSYE**: Deep sternal wound site infection, **HDTI**: Superficial sternal wound infection

The length of ICU stay of patients in group S was statistically significantly shorter than that of patients in group P (Figure 8).

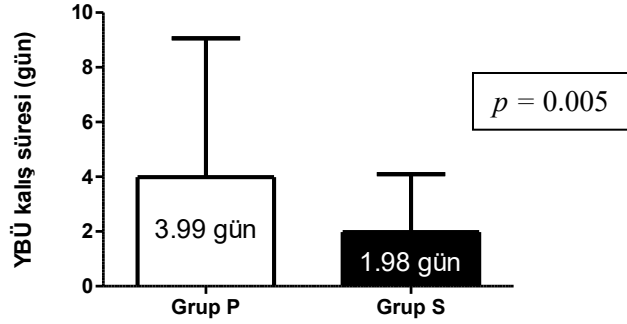


Figure 8: Evaluation of the groups in terms of length of ICU stay

Patients in group S had a statistically significantly shorter hospital stay than patients in group P (Figure 9).

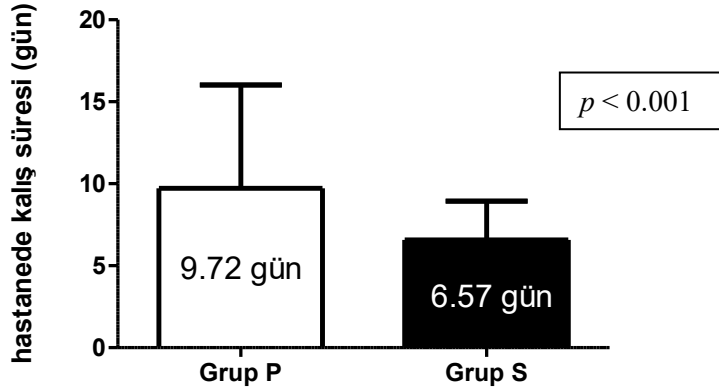


Figure 9: Evaluation of the groups in terms of length of hospital stay

Discussion

The data obtained were evaluated in terms of their effects on postoperative drainage. There was no statistically significant difference in preoperative heparin use. In 41.7% of the patients in the pedicled IMA removal group and 40.7% of the patients in the skeletonized IMA removal group, heparin was used preoperatively. There was no statistically significant difference in the use of protamine and transamine in the postoperative intensive care unit. Postoperative heparin use was statistically significantly higher in the skeletonized IMA removal group than in the pedicled group ($p = 0.012$). Heparin was used in 8% of patients in group P and 20.4% in group S in the postoperative period. The correlation between the number of distal anastomoses performed intraoperatively and postoperative drainage was not statistically significant. The number of coronary vessels bypassed during the operation did not statistically significantly affect the amount of drainage in this study. There was a positive correlation between the presence of plaque in the revascularized LAD and postoperative heparin use. Similarly, the correlation between case exit ACT value and postoperative drainage was not statistically significant.

Calafiore A. M. et al. in their study comparing the mid-term results of pedicled and skeletonized conduits in patients with bilateral internal mammary artery removal compared the 12-hour mean drainage of patients with skeletonized and pedicled conduits and found that drainage was statistically significantly less in the skeletonized group (674 ± 531 mL/12h versus 542 ± 306 mL/12h $p = 0.001$) (Calafiore et al., 1999). In our study, the mean total drainage of patients in group P was statistically significantly higher than that of patients in group S (1064.72 ± 537.88 mL vs. 850.00 ± 382.77

mL; $p = 0.007$). Similarly, the mean drainage of patients in group P on the first postoperative day was statistically significantly higher than that of patients in group S (303.68 ± 203.71 mL vs. 129.63 ± 129.77 mL; $p < 0.001$). The mean drainage amount on the second day was similarly higher in patients with pedicled conduit (91.72 ± 193.98 mL vs. 22.22 ± 67.76 mL; $p = 0.011$). Despite these results, the mean drainage amount on the day of surgery in both groups was close to each other, but slightly higher in Group S (652.76 ± 296.82 mL vs. 688.89 ± 315.73 mL; $p = 0.409$). Although the total drainage amount and the drainage amounts on the first and second postoperative days were significantly lower in the group using skeletonized IMA, they were higher on the day of surgery compared to the pedicled group, which necessitated further research. There was a low correlation between patients with plaque LAD and postoperative heparin use in the pedicled IMA group. In the group using skeletonized IMA, there was a moderate correlation between patients with plaque LAD and postoperative heparin use. In group S, more heparin was used postoperatively in patients with plaque LAD. Therefore, postoperative heparin use was found to be statistically significantly higher in group S. When preoperative data were evaluated, it was found that the mean weight of patients in group S was statistically significantly higher than that of patients in group P (80.22 ± 10.78 kg vs. 75.64 ± 13.68 kg; $p = 0.026$). In addition, postoperative redistribution of intraoperative heparin would be greater in the skeletonized group with a higher mean weight. This is an important factor such as postoperative heparin use in terms of increasing the amount of drainage on the day of surgery. In addition, although there was no statistically significant difference when the amount of drainage on the day of surgery was compared to body

weight, there was less drainage per kilogram in the skeletonized IMA group ($9.35 \pm 7.80\text{mL/kg}$ vs. $8.80 \pm 4.63\text{mL/kg}$; $p = 0.627$).

Eight patients (4.9%) in group P underwent bleeding revision on the day of surgery, while 1 patient (1.9%) in group S underwent bleeding revision ($p = 0.329$). At postoperative follow-up, 2 patients (1.2%) in the pedicled conduit removal group were re-operated due to tamponade, whereas no patients in the skeletonized conduit removal group were re-operated ($p = 0.413$).

Patients who receive blood transfusions may experience different complications ranging in severity from febrile non-hemolytic reactions to anaphylactic reactions. Patients may show a simple symptom such as fever, or they may face life-threatening shock, or they may struggle with the HIV virus transmitted during transfusion for the rest of their lives. Therefore, it is very important to administer as little postoperative blood transfusion as possible in order to protect patients from possible risks. In their study, Peterson et al. showed that patients using skeletonized grafts needed less blood transfusion than patients using pedicled grafts (Peterson et al., 2003). Calafiore A. M. et al. also showed that fewer patients in the group with skeletonized IMA removal needed blood transfusion (Calafiore et al., 1999). In our study, statistically significantly fewer blood transfusions were administered in the skeletonized group (1.50 ± 1.24 U vs. 2.88 ± 2.29 U; $p < 0.001$).

In a study conducted by Onorati et al. in 2007, they found a higher incidence of superficial wound site complications in the pedicled IMA removal group (Onorati et al., 2007). They said that the incidence of deep wound site complications was also comparable. Peterson et al. also found an unacceptably high rate of

deep sternal wound infection in diabetic patients undergoing bilateral pedicled IMA removal (Peterson et al.,2003). In patients with skeletonized bilateral IMA removal, this rate was found to be comparable to non-diabetic patient groups. The prevalence of superficial or deep sternal wound infection was also found to be lower in the skeletonized conduit preparation group. In our study, deep sternal wound infection was seen in 9 patients (5.6%) in the pedicled conduit group, whereas no deep wound infection was seen in the skeletonized group. Superficial sternal wound infection was found to have a statistically significant higher prevalence in the pedicled group. 29 patients (17.9%) versus 3 patients (5.6%); $p = 0.027$]. With the skeletonized technique, the collaterals of the sternal and anterior intercostal branches are preserved during IMA removal. In this way, sternal blood flow is maintained.

Calafiore et al. and Peterson et al. separately reported shorter intensive care unit stay and shorter hospital stay in the skeletonized IMA removal group compared to the pedicled IMA removal group (Calafiore et al.,1999; Peterson et al.,2003). In the present study, the duration of intensive care unit stay was statistically significantly shorter in the skeletonized group (3.99 ± 5.07 days versus 1.98 ± 2.12 days; $p = 0.005$). The mean hospital stay was also significantly shorter in the skeletonized conduit group than in the pedicled conduit group (6.57 ± 2.37 days versus 9.72 ± 6.30 days; $p < 0.001$). The fact that the amount of drainage is higher in the group using pedicled conduits causes the drains to be withdrawn later, thus increasing the duration of intensive care and therefore hospital stay.

Conclusion

Long-term patency rates of grafts used in myocardial revascularization are very important in terms of both long-term survival and comfort of life. Considering these issues, arterial grafts, especially IMA as the gold standard, have been widely used in coronary artery bypass surgery. In this study comparing the early postoperative outcomes of two different patient groups using IMAs harvested with pedicled and skeletonized techniques, it was found that the skeletonized technique significantly reduced the total postoperative drainage.

The meticulousness and precision required in the application of the skeletonized technique positively affects hemostasis. In the skeletonized technique, the collateral veins and side branches are not touched unless specifically required for widening the field of view and freeing the IMA. In addition, since the side branches of the IMA are visualized and removed using the double clip technique, the risk of bleeding due to side branches is reduced. Accordingly, patients using skeletonized grafts required less blood transfusion in the postoperative period. Likewise, the intensive care unit and hospital stay of patients with skeletonized conduit were shorter than the pedicled group. All these factors suggest that the use of the skeletonized technique for IMA release is more advantageous for the patient. Serious complications due to bleeding complications of the internal mammary artery can be significantly reduced with the skeletonized technique, which will also reduce hospital costs.

References

Henriquez-Pino, J., Gomes, W., Prates, J., & Buffolo, E. (1997). Surgical anatomy of the internal thoracic artery. *Annals of Thoracic Surgery*, 64(4), 1041-1045.

Notes from Ankara University Faculty of Medicine, Department of Cardiovascular Surgery. Conduits used in coronary artery bypass surgery. Retrieved from www.medicine.ankara.edu.tr/cerrahi_tip/kvc/modules

De Jesus, R., & Acland, R. (1995). Anatomic study of the collateral blood supply of the sternum. *Annals of Thoracic Surgery*, 59(1), 163-168.

Arnold, M. (1972). The surgical anatomy of sternal blood supply. *Journal of Thoracic and Cardiovascular Surgery*, 64(4), 596-610.

Seyfer, A., Shriver, C., Miller, G., & Graeber, G. (1988). Sternal blood flow after median sternotomy and mobilization of the internal mammary arteries. *Surgery*, 104(5), 899-904.

Calafiore, A., Vitolla, G., Iaco, A., Fino, C., Di Giammarco, G., Marchesani, F., et al. (1999). Bilateral internal mammary artery grafting: Midterm results of pedicled versus skeletonized conduits. *Annals of Thoracic Surgery*, 67(6), 1637-1642.

Onorati, F., Esposito, A., Pezzo, F., Di Virgilio, A., Mastroberto, P., & Renzulli, A. (2007). Hospital outcome analysis after different techniques of left internal mammary grafts harvesting. *Annals of Thoracic Surgery*, 84(3), 912-919.

Peterson, M., Borger, M., Rao, V., Peniston, C., & Feindel, C. (2003). Skeletonization of bilateral internal thoracic artery grafts lowers the risk of sternal infection in patients with diabetes. *Journal of Thoracic and Cardiovascular Surgery*, 126(5), 1314-1319.

Pevni, D., Mohr, R., Lev-Ran, O., Paz, Y., Kramer, A., Frolkis, I., et al. (2003). Technical aspects of composite arterial grafting with double skeletonized internal thoracic arteries. *Chest*, 123(4), 1348-1354.

Tatoulis, J., Buxton, B., & Fuller, J. (1997). Results of 1,454 free right internal thoracic artery-to-coronary artery grafts. *Annals of Thoracic Surgery*, 64(5), 1263-1268.

CHAPTER II

Early detection of cardiovascular disease using deep learning technique

Harun SELVİTOPI¹
Seda DEMİR²

INTRODUCTION

The cardiovascular diseases (CVD) is one of the most important case for the mortality and morbidity in the worldwide. It causes the nearly 30 % percentage of the dead in the world every year.

The early detection of the cardiovascular diseases is critical step for the safe of the patient. For this purpose, the deep learning and machine learning techniques have been used to diagnosis the early stage of the CVD's. In (Rustam, 2022: 1474), the convolutional

¹Associate Professor, Erzurum Technical University, Mathematics, Orcid: 0000-0001-5958-7625, harun.selvitopi@erzurum.edu.tr

²Research Assistant, Erzurum Technical University, Mathematics, Orcid: 0000-0003-0655-9326, seda.demir@erzurum.edu.tr

neural network (CNN) has been applied to early diagnosis of the CVD. The combination of the CNN with LSTM deep learning methods has been proposed to analyze the clinical data for the early prediction of CVD in (Hossain, 2023: 101370). In (Khozeimeh, 2022: 11178), the random forest with convolutional neural network has been proposed to analyze the coronary artery disease dataset to predict the disease. The CNN has been applied to CVD dataset to early detection in (Sajja, 2020: 601-606). In (Dutta, 2020: 113408), the CNN has been applied to imbalanced dataset for the prediction of the CVD. The convolutional neural network has been considered to detect the heart disease and compared with the other machine learning methods in (Shankar, 2020: 170). In (Jain, 2023: 119859) the Levy flight-Convolutional Neural Network combine method has been used to diagnosis the coronary heart disease. The CNN has been considered to diagnosis of the HF in (Mehmood, 2021: 3409-3422).

In this study, we have been considered the Sathvi hybrid dataset to analyze using convolutional neural network and we have been compared the obtained evaluation metrics with machine learning methods as: Logistic Regression (LR), k-nearest neighbour (k-NN) and Random Forest Classifier (RFC).

DEEP LEARNING AND MACHINE LEARNING ALGORITHMS

This section provides a brief overview of the machine learning algorithms employed in this study.

Convolutional Neural Network

Convolutional Neural Network (CNN) is a deep learning model specifically designed to analyze structured grid data, like

images. It leverages multiple layers, including convolutional, pooling, and activation layers, to automatically identify and extract features from the input. This makes CNNs highly effective for tasks such as image classification and pattern recognition. Their ability to learn spatial relationships between features makes them particularly well-suited for applications in computer vision.

Logistic Regression

Logistic regression is a statistical technique primarily used for binary classification, where the objective is to predict one of two possible outcomes. It establishes a relationship between one or more independent variables and a binary dependent variable, such as yes/no or true/false. The model employs the logistic (sigmoid) function to convert the result of a linear equation into a probability ranging from 0 to 1. This probability indicates the likelihood of an input belonging to a specific class. If the probability is greater than a chosen threshold (usually 0.5), the model predicts the positive class; otherwise, it predicts the negative class. Due to its simplicity, ease of interpretation, and effectiveness, logistic regression is widely applied in areas like healthcare, finance, and social science research.

k-Nearest Neighbour

The k-Nearest Neighbors (k-NN) algorithm is a simple and intuitive machine learning technique used for both classification and regression tasks. It works by determining the class or value of a data point based on the 'k' closest data points in the training set, where 'k' is a user-defined parameter specifying how many neighbors to consider. In classification, k-NN assigns the data point to the most common class among its 'k' nearest neighbors. In regression, it predicts the value by averaging (or weighted averaging) the values

of the nearest neighbors. As a non-parametric method, k-NN doesn't assume any specific distribution of the data, making it adaptable to a wide range of applications, such as pattern recognition, image classification, and recommendation systems. However, despite its simplicity and effectiveness, k-NN can be computationally expensive for large datasets, as it requires calculating the distance between the query point and every point in the training set.

Random Forest Classifiers

Random Forest classifiers are an ensemble learning method used for both classification and regression tasks. This technique involves constructing multiple decision trees during training and combining their predictions to improve accuracy and reliability. The core idea of Random Forest is to create a "forest" of decision trees, each trained on a random subset of the data. This approach reduces overfitting and enhances the model's ability to generalize to unseen data. Each decision tree is built using a random sample from the training data, and at each split in the tree, a random subset of features is selected. This randomness ensures diversity among the trees, minimizing the correlation between them. For making predictions, the Random Forest classifier aggregates the outputs from all the trees. In classification tasks, it uses the majority vote across all trees to determine the final class, while for regression, it averages the predictions of all trees. Random Forest is widely used because it performs well with large datasets containing many features and is less prone to overfitting than individual decision trees. Additionally, it is easy to use and interpret, making it suitable for various applications, including fraud detection, bioinformatics, and customer segmentation.

DATA

The "Hybrid" and "Sathvi" datasets, containing 920 and 531 instances respectively, are provided as supplementary materials in (Kanagarathinam, 2022: 102042). The "Sathvi" dataset, which is complete with no missing values, was used to develop the CVD risk prediction model.

Sathvi Dataset

The "Hybrid" dataset combines four distinct datasets—Hungarian, Switzerland, Cleveland, and Long Beach—into one unified dataset, containing 920 instances, each with 14 attributes. However, there are 621 missing values per instance within this dataset. Specifically, more than 50% of the values for the 'ca' and 'thal' features are missing, leading to the removal of these two columns to form a new dataset called "Sathvi." Furthermore, any instances with missing values in the "Hybrid" dataset were excluded. As a result, the final "Sathvi" dataset consists of 531 instances and 12 features, with no missing values. The processed "Hybrid" and "Sathvi" datasets are in the supplementary file.

MEASURES OF PERFORMANCE EVALUATION

The performance of the proposed models was evaluated using five metrics: specificity, precision, accuracy, recall, and F-measure.

$$Accuracy = \frac{TP + TN}{TP + TN + FP + FN}$$

$$Recall = \frac{TP}{TP + FN}$$

$$Precision = \frac{TP}{TP + FP}$$

$$F1score = \frac{2xTP}{2xTP + FN + FP}$$

$$Specificity = \frac{TN}{TN + TP}$$

where TP = True positive rate, TN = True negative rate, FP = False positive rate, FN = False negative rate.

RESULTS AND DISCUSSION

In this study, deep learning technique convolutional neural network and machine learning techniques such as k-nearest neighbors, logistic regression, and Random Forest Classifier were employed to analyze the Sathvi dataset for diagnosing cardiovascular diseases. The performance of these methods was evaluated using various metrics, including accuracy, precision, recall, and the F1 score, all derived from the confusion matrix, as shown in Table 1.

Table 1: The accuracy, precision, recall and F1-score of the Machine Learning methods.

Method	Accuracy (%)	Precision (%)	Recall(%)	F1-Score (%)
CNN	83.18	84.00	89.00	87.00
Logistic Regression	81.88	88.24	84.11	86.12
k-NN	80.00	88.24	81.82	84.91
Random Forest Classifier	77.50	86.28	80.00	83.02

As shown in Table 2, the proposed methods achieved accuracy, precision, recall, and F1-Score values of 83.18%, 84.00%, 89.00%, and 87.00%, respectively. These results demonstrate the effectiveness of the methods in detecting cardiovascular diseases.

KAYNAKÇA

Rustam, F., Ishaq, A., Munir, K., Almutairi, M., Aslam, N., & Ashraf, I. (2022). Incorporating cnn features for optimizing performance of ensemble classifier for cardiovascular disease prediction. *Diagnostics*, 12(6), 1474. doi: 10.3390/diagnostics12061474

Hossain, M. M., Ali, M. S., Ahmed, M. M., Rakib, M. R. H., Kona, M. A., Afrin, S., ... & Rahman, M. H. (2023). Cardiovascular disease identification using a hybrid CNN-LSTM model with explainable AI. *Informatics in Medicine Unlocked*, 42, 101370. doi:10.1016/j.imu.2023.101370

Khozeimeh, F., Sharifrazi, D., Izadi, N. H., Joloudari, J. H., Shoeibi, A., Alizadehsani, R., ... & Islam, S. M. S. (2022). RF-CNN-F: random forest with convolutional neural network features for coronary artery disease diagnosis based on cardiac magnetic resonance. *Scientific reports*, 12(1), 11178. doi: 10.1038/s41598-022-15374-5

Sajja, T. K., & Kalluri, H. K. (2020). A Deep Learning Method for Prediction of Cardiovascular Disease Using Convolutional Neural Network. *Rev. d'Intelligence Artif.*, 34(5), 601-606. doi:10.18280/ria.340510

Dutta, A., Batabyal, T., Basu, M., & Acton, S. T. (2020). An efficient convolutional neural network for coronary heart disease prediction. *Expert Systems with Applications*, 159, 113408. doi: 10.1016/j.eswa.2020.113408

Shankar, V., Kumar, V., Devagade, U., Karanth, V., & Rohitaksha, K. (2020). Heart disease prediction using CNN

algorithm. *SN Computer Science*, 1(3), 170. doi: 10.1007/s42979-020-0097-6

Jain, A., Rao, A. C. S., Jain, P. K., & Hu, Y. C. (2023). Optimized levy flight model for heart disease prediction using CNN framework in big data application. *Expert Systems with Applications*, 223, 119859. doi: 10.1016/j.eswa.2023.119859

Mehmood, A., Iqbal, M., Mehmood, Z., Irtaza, A., Nawaz, M., Nazir, T., & Masood, M. (2021). Prediction of heart disease using deep convolutional neural networks. *Arabian Journal for Science and Engineering*, 46(4), 3409-3422. doi: 10.1007/s13369-020-05105-1

Kanagarathinam, K., Sankaran, D., & Manikandan, R. (2022). Machine learning-based risk prediction model for cardiovascular disease using a hybrid dataset. *Data & Knowledge Engineering*, 140, 102042. doi: 10.1016/j.datak.2022.102042

CHAPTER III

Mesothelioma

Aykut ELİÇORA¹

Intraduction

The presence of 5-15 mL of fluid in the pleural space is considered normal and it is thought that this fluid facilitates the sliding of the pleural sheets over each other during the respiratory cycle. (Çobanoğlu & et al, 2017) Fluid accumulation between the pleural membranes due to various reasons is called pleural effusion (PE). Pleural effusion may occur with increased production or decreased drainage of pleural fluid. Especially malignant processes can cause recurrent pleural effusions and repeated hospitalizations.

Primary tumors or metastases of the pleura disrupt pleural lymphatic drainage and this causes a gradual increase in pleural fluid. The most common tumors that cause pleural metastasis are

¹ Doç. Dr.Aykut Eliçora ,Kocaeli Üniversitesi, Tıp Fakültesi, Göğüs Cerrahisi Bölümü, Kocaeli/Türkiye, Orcid: 0000-0002-9565-0692 aykutelicora@yahoo.com.tr

bronchogenic carcinomas (40%) and breast cancer (25%). Mesothelioma, the primary malignant tumor of the pleura, causes malignant pleural effusion with a frequency of 9% among all malignancies. Malignant pleural mesothelioma is the most common primary malignancy of the pleura. In addition to all these malignant effusions, decreased intravascular oncotic pressure due to various reasons, widespread ascites in the abdomen and systemic insufficiencies may also be involved in the etiology of pleural effusion. (Çobanoğlu & et al, 2017; Şenyiğit, 2011)

Investigating the etiology of pleural effusion is very important to start treatment directed to the etiology. In determining the etiology of pleural effusion, pathology, culture, biochemistry, hemogram and AFB staining should be performed on the fluid taken by thoracentesis. Especially in the cytological examination performed in PE, showing malignant cells shed into the fluid from tumors that create an obstructive effect on lymphatic drainage is very important in terms of staging. (Çobanoğlu & et al, 2017)

Depending on the amount of pleural effusion, different clinical conditions may occur. In particular, the filling of one hemithorax with effusion and the displacement of mediastinal structures towards the opposite hemithorax is defined as mediastinal shift. Due to this mediastinal shift, compression of the opposite lung and decreased cardiac input may occur, leading to clinical conditions ranging from respiratory arrest.

Etiology of malignant mesothelioma

Asbestos fibers are present in the etiology of malignant mesothelioma (MM), the primary malignant tumor of the pleura. These asbestos fibers are divided into two main groups: serpentine

and amphibole (Crosidolite). Another subtype of asbestos, erionite, also plays a role in the development of malignancy. The presence of these crystals in a fibrous structure facilitates the inhaled crystals to pass through the lungs and settle in the pleura. (Şahin & et al, 2020; Tanrıverdi & et al, 2021)

These crystals, taken in by inhalation, first pass into the terminal airways, and from there into the pleural cavity, where they become trapped. They can remain latent here and cause benign asbestos plaques, as well as the development of malignancy through inflammatory processes. Although rare, MM can develop in patients receiving radiotherapy for the treatment of any malignancy, although the mechanism has not been fully elucidated, without exposure to asbestos (Şahin & et al, 2020).

Demographic characteristics

Malignant mesothelioma is more common in men (M/F= 5:1). This gender difference is due to occupational exposures. The disease remains latent for a long time after exposure and occurs more frequently in the 5th-6th decades. During this long period, it is thought that asbestos crystals create a cytotoxic effect on mesothelial cells, initiate inflammatory processes, trigger the expression of proto-oncogenes and ultimately cause malignancy. Although the name mesothelioma first brings to mind pleural mesothelioma; it can also be seen in the pericardium, peritoneum and testis in addition to the pleura.

Clinical

The disease, which presents with chest pain, cough and dyspnea, can progress rapidly. Pleuritic pain is most commonly seen due to the involvement of the pleural membranes. Arm pain,

abdominal pain, etc. can also be seen with the invasion of the tumor into the surrounding tissues. This pleuritic pain can be a severe pain that does not respond to analgesics. Some advanced cases may show B symptoms (Table 1). Dyspnea caused by PE may appear as an earlier presenting symptom than pain. The incidence of PE at any stage of the disease has been reported as 95%. Lung restriction secondary to pleural thickening, such as pulmonary atelectasis secondary to PE, is also one of the causes of dyspnea. Although it starts locally, it may spread to the myocardium, intestines and lung tissue in advanced stages; ascites and chest deformity may also be seen in these patients. (Hajj & et al, 2021; Şenyiğit, 2011; Ökten & et al, 2013; Tanrıverdi & et al, 2021; Hajj & et al, 2021)

In malignant mesothelioma, involvement in the right hemithorax is seen more frequently (60%). (Hajj & et al, 2021; Şenyiğit, 2011)

Table 1: B symptoms

B symptoms
<ul style="list-style-type: none"> • weight loss (>10% of body weight in the last 6 months) • non-infective, persistent fever • night sweats

Asbestos crystals accumulate in the lower half of the hemithorax under the effect of gravity. Therefore, it is thought that MM first appears in the lower half of the hemithorax. Since MM shows regional spread, surgical interventions for diagnosis or

treatment may cause tumor cells to seed the surrounding tissue. Again, due to this regional spread feature; the adjacent pericardium and hemidiaphragm are also affected by the disease. These tissues lose their flexibility after tumor invasion and a restrictive structure forms around the lung. Another reason for dyspnea in the later stages of MM is this physiopathological mechanism (Ökten & et al, 2013).

Diagnosis

Since recurrent pleural effusions may be caused by MM, it should be kept in mind that even if a mass formation is not noticeable in the imaging at the beginning of the disease, a cytological diagnosis of MM can be made in this patient group. Sometimes, when the pleura is examined exploratively, pleural lesions that have not yet been noticed in the imaging can be detected. However, since the complaints at the early stage are nonspecific and no obvious lesions are detected, reaching the diagnosis may not be as fast as desired in clinical practice. Considering all these, it can be accepted that the first diagnostic method is thoracentesis and cytological examination. Exposure should be questioned in the anamnesis and MM should be considered. Nevertheless, diagnosis can only be reached in 30-50% of patients with this method (Ökten & et al, 2013).

Findings such as unilateral pleural effusion, volume reduction in one hemithorax, mediastinal widening, and hydropneumothorax on chest radiography should raise suspicion of MM and the etiology should be investigated with advanced imaging methods. Pleural thickening greater than 1 cm, pleural irregularities or nodules, and pleural plaques can be seen on the affected side on thorax CT. In this case, PET and textural sampling are recommended (Figure 1) (Şenyiğit, 2011).

Pleural effusion in MM is an exudative fluid rich in lymphocytes and proteins, with high LDH levels. When examined macroscopically, it may give the impression of hemorrhage. In microscopy, atypical mesothelial cells can be seen to cluster in places due to tumoral involvement or secondary to interventional procedures. A cell block is needed for immunohistochemistry to be performed for diagnosis. This situation requires more interventional diagnostic methods. In recent years, percutaneous pleural biopsies performed with imaging guidance provide diagnosis at a rate of almost 80%. Due to the diagnostic difficulty of MPM, studies on the diagnosticity of some biomarkers such as mesothelin, osteopontin, periostin, YKL-40 (chitinase-like protein), tenascin-c, IDO (indolamine 2,3-dioxygenase) and fibulin-3 are ongoing. (Ökten & et al, 2013; Tanrıverdi & et al, 2021). There are four histological subtypes of MM: epithelial, sarcomatoid, mixed (biphasic) and desmoid. The prognosis of the sarcomatoid and mixed types is worse. Since the sarcomatoid type has less desquamation, it is less diagnostic than pleural effusion. Histopathologically, it may be difficult to distinguish MPM from the more benign hyperplastic mesothelia or pleural adenomatoid tumor. Immunohistochemical BAP1 positivity and CDKN2A deletion are evaluated for differential diagnosis.

In the early stages, percutaneous sampling has a lower diagnostic value, and in case of clinical suspicion, perioperative pleural sampling can also be considered. In this case, video-assisted thoracoscopic surgery (VATS) provides comfort to the patient and the surgeon, and can shorten hospital stays. VATS is superior to percutaneous biopsies performed directly or with imaging in terms of being able to visually sample lesions, obtaining multiple samples

in a single session, and observing the entire pleura, including the mediastinal pleura. It is recommended to obtain samples from at least 5 different localizations in order to obtain a sufficient number of samples. In this way, an idea is obtained about the relationship of the disease with the surrounding tissue and its spread. In addition, decortication and mechanical/chemical pleurodesis can be performed in the same session. In both MM and metastatic adenocarcinoma, gray/yellow/white nodules that tend to merge on the pleural surfaces can be seen. Although the need for thoracotomy has decreased in the presence of VATS, it is partially preferred, especially in patients with intense pleural adhesions. However, the need for a more specific anesthesia in thoracotomy, prolonged hospital stay, and increased local spread of the tumor are negative aspects compared to VATS. (Ökten & et al, 2013; Şenyiğit, 2011)

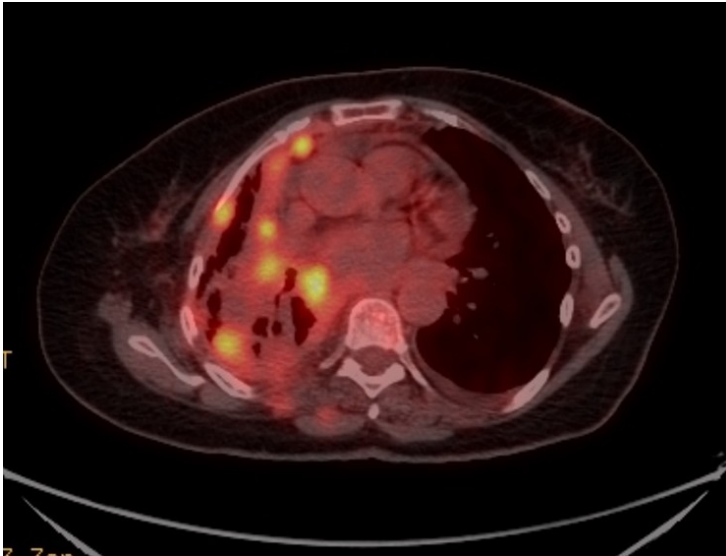


Figure 1: PET-CT image of a case diagnosed with mesothelioma after pleural biopsy with VATS.

Staging

There is still no currently accepted staging system in MM that has been associated with survival. The rapid progression of the disease may be the main reason for this. The expected follow-up after diagnosis is predicted to be 12 months. (Ökten & et al, 2013; Şahin & et al, 2020) The ninth thoracic oncology staging published by IASLC (International Association for the Study of Lung Cancer) in 2024 is used (Tables 2,3). FDG-18 PET-CT is recommended for staging the lesion. In patients with a chance of operability; MRI can also be examined due to its high sensitivity. CT and PET are routinely used for operability and follow-up purposes. (Hajj & et al, 2021)

Table 2: IASLC 9th; Class T

TClass)	Clinical T (cT)	Pathological T (pT)
T1	<p>Tumor is limited to the ipsilateral pleura</p> <p>$P_{sum} \leq 12$ mm and no fissure involvement</p> <p>($F_{max} \leq$ mm)</p>	<p>Tumor is limited to the ipsilateral pleura and no fissure involvement</p>
T2	<p>Tumor invades ipsilateral pleura; $P_{sum} \leq 12$ mm and one of the following:</p> <ul style="list-style-type: none"> • $F_{max} > 5$ mm, fissure invasion • Mediastinal fatty tissue invasion • Single site, soft tissue invasion of chest wall <p>Or</p> <p>Tumor invades ipsilateral pleura > 12 mm and ≤ 30 mm. May or may not be:</p> <ul style="list-style-type: none"> • $F_{max} > 5$ mm, fissure invasion • Mediastinal fatty tissue invasion • Single site, soft tissue invasion of chest wall 	<p>The tumor has invaded the ipsilateral pleura and has one of the following:</p> <ul style="list-style-type: none"> • Fissure invasion • Ipsilateral lung parenchyma invasion • Diaphragm (non-transmural) invasion

T3	<p>Tumor invades ipsilateral pleura, Psum> 30 mm; may or may not have:</p> <ul style="list-style-type: none"> • Fmax> 5 mm, fissure invasion • Mediastinal fatty tissue invasion • Single site, soft tissue invasion in the chest wall 	<p>Tumor is limited to ipsilateral pleura. Fissure invasion may or may not occur. Invasion of one of the following:</p> <ul style="list-style-type: none"> • Mediastinal fatty tissue • Surface of pericardium • Endothoracic fascia • Soft tissue invasion in a single area of the chest wall
T4	<p>At any tumor size, there is involvement of one of the following:</p> <ul style="list-style-type: none"> • Chest wall bones (ribs) • Mediastinal organs (heart, spine, esophagus, trachea, great vessels) • Diffuse involvement of the chest wall • Direct tumor extension through the diaphragm or pericardium • Direct extension to the contralateral pleura • Presence of malignant pericardial effusion 	<p>There is invasion of one of the following:</p> <ul style="list-style-type: none"> • Chest wall bones (ribs) • Mediastinal organs (heart, spine, esophagus, trachea, great vessels) • Diffuse involvement of the chest wall • Transmural involvement of the diaphragm or pericardium • Direct extension to the contralateral pleura • Presence of malignant pericardial effusion

Table 3: IASLC 9th; Class N

N Class	Clinical and Pathological Definition
N0	No regional lymph node metastasis
N1	Ipsilateral intrathoracic lymph node involvement <ul style="list-style-type: none"> • Bronchopulmonary, hilar, subcarinal, paratracheal, aortopulmonary, paraesophageal, peridiaphragmatic • Ipsilateral pericardial fatty tissue • Ipsilateral intercostal and internal mammary LN
N2	Metastasis to contralateral lymph nodes, metastasis to ipsilateral or contralateral supraclavicular lymph nodes

Treatment

There is no treatment modality that clearly contributes to survival yet (Ökten & et al, 2013). Although single and double treatment modalities have been tried in MM, they have not been successful. Therefore, treatment modalities that combine surgery, chemotherapy and radiotherapy are also being tried today. (Tanrıverdi & et al, 2021; Yüksel & Balcı, 2015; Hajj & et al, 2021) Systemic chemotherapy does not provide a full response, and generally 15-20% respond to treatment. In radiotherapy, irradiation of a large area causes toxicity. In surgical interventions, the possibility of transplantation and recurrence is high. Considering all

these, the treatment of malignant pleural mesothelioma is still a situation that needs to be studied.

In surgical treatment, extrapleural pneumonectomy (extended pleuropneumectomy) (EPP) is performed. Before that, echocardiography (ECHO) should be performed to determine the status of the pericardium and ventricles. As in all lung resections, preoperative respiratory reserve should be carefully evaluated. In surgical terms; Pleurectomy/Decortication (P/D) is recommended as an alternative to EPP in patients with limited respiratory reserve, low cardiopulmonary reserve or who are thought to be in the early stage radiologically. The limitations of the surgical method are that even in diagnostic procedures, Malignant Pleural Mesothelioma is seeded in the surrounding tissue and that it cannot be proven that the disease is microscopically limited or completely resected (Yüksel & Balcı, 2015). When the contribution of extrapleural pneumonectomy and decortication to the survey is compared; A 1.4-fold increased risk of death was observed in patients who underwent extrapleural pneumonectomy (Hajj & et al, 2021).

REFERENCES

1. Çobanoğlu, U., Kızıltan, R., & Kemik, Ö. Malignant Pleural Efusions: Diagnosis and Treatment. Van Med J. 2017; 24(4): 397-403 | DOI: 10.5505/vtd.2017.96967
2. Hajj GNM, Cavarson CH, Pinto CAL, Venturi G, Navarro JR, Lima VCC. Malignant pleural mesothelioma: an update. J Bras Pneumol. 2021 Dec 13;47(6):e20210129. doi: 10.36416/1806-3756/e20210129
3. Şenyiğit A : Clinical assesment and variations at malignant mesotelioma. Türk Toraks. 2011 Nov, 142-145 doi:10.5152/pb.2011.14
4. Ökten İ, Kavukçu HŞ, Turna A, Eroğlu A, Kayı Cangır A (2013): Göğüs Cerrahisi, 1573-1583. İstanbul: İstanbul Tıp
5. Şahin E, Kosif A, Kargı B (2020): Plevranın Malign Hastalıkları, 1-25. Ankara: Nobel
6. <https://www.iaslc.org/research-education/publications-resources-guidelines/staging-cards-thoracic-oncology-9th-edition>
7. Tanrıverdi Z, Meteroglu F, Yüce H, Şenyiğit A, Işcan M, Ünüvar S. The usefulness of biomarkers in diagnosis of asbestos-induced malignant pleural mesothelioma. Hum Exp Toxicol. 2021 Nov;40(11):1817-1824. doi: 10.1177/09603271211017324.
8. Yüksel M, Balcı AE (2015): Kırmızı Kitap, 517-528. İstanbul: Nobel

9. Popat S, Curioni-Fontecedro A, Dafni U, Shah R, O'Brien M, Pope A, Fisher P, Spicer J, Roy A, Gilligan D, Gautschi O, Nadal E, Janthur WD, López Castro R, García Campelo R, Rusakiewicz S, Letovanec I, Polydoropoulou V, Roschitzki-Voser H, Ruepp B, Gasca-Ruchti A, Peters S, Stahel RA. A multicentre randomised phase III trial comparing pembrolizumab versus single-agent chemotherapy for advanced pre-treated malignant pleural mesothelioma: the European Thoracic Oncology Platform (ETOP 9-15) PROMISE-meso trial. *Ann Oncol.* 2020 Dec;31(12):1734-1745. doi: 10.1016/j.annonc.2020.09.009. Epub 2020 Sep 22.

CHAPTER IV

Carcinoid Tumor: A Rare Primary Bone Localization? Bone Metastasis?

Mertay Boran¹
Mohammed Jebeli²
Reşad Kızıllok³
Asuman Kilitçi⁴

INTRODUCTION:

Carcinoid tumors, which are a subset of neuroendocrine tumors, are typically slow-growing and arise from the neuroendocrine cells of various organs. The most common locations for these tumors are the gastrointestinal (GI) tract (58-75%) and the lungs (20-31%), though carcinoid tumors have been identified in

¹ MD , Duzce University, Thoracic Surgery, Orcid: 0000-0002-9027-6988

² Dr, Duzce University, Medicine, Orcid:0009-0009-3516-5693

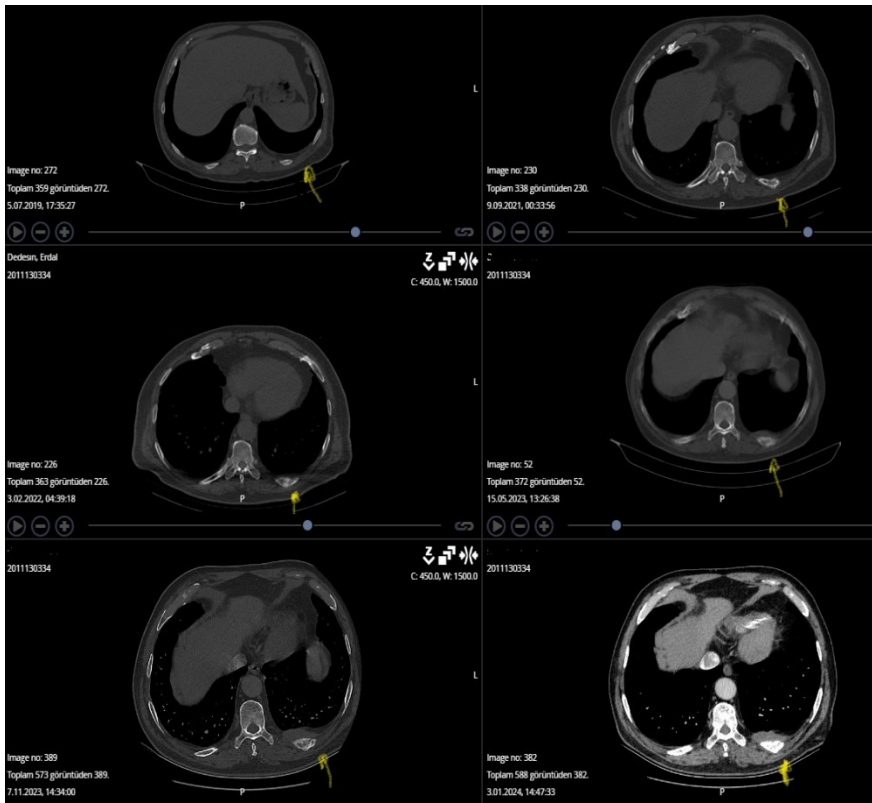
³Dr, Üniversite, Bölüm, Orcid:0009-0006-2750-9239

⁴ Associate professor, Duzce University, Pathology, Orcid: 0000-0002-5489-2222

other rarer sites such as the pancreas, liver, bile ducts, esophagus, pancreas, gallbladder, uterine servix, testis, middle ear, larynx breast and ovaries. (Moddlin, 2003, 934-959) Bone involvement by carcinoid tumors is exceedingly rare, and the majority of carcinoid metastases typically spread to the liver, lungs, and lymph nodes, with skeletal metastasis occurring in a small percentage of cases.(İncekara, 2018,304; Moddlin ,2005, 92–101) This case report highlights the rare occurrence of an atypical carcinoid tumor in the rib, which was further complicated by the presence of a coexisting schwannoma in the leg. It also discusses the challenges associated with diagnosis and management, as well as the importance of re-evaluating previous medical findings, such as a gallbladder pathology, in the context of complex tumor presentations.

CASE PRESENTATION:

A 65-year-old male with a history of type 2 diabetes, hypertension, and partial cholecystectomy (gallbladder removal) performed one year prior, presented with a three-year history of persistent left-sided chest pain. Initially, the symptoms were thought to be musculoskeletal in origin. However, a CT scan of the chest performed in 2021 revealed a lesion in the left 10th rib, which was initially interpreted as a pathological fracture. Over the following two years, the lesion grew significantly in size (52x20 mm), prompting concerns about malignancy (Picture 1).



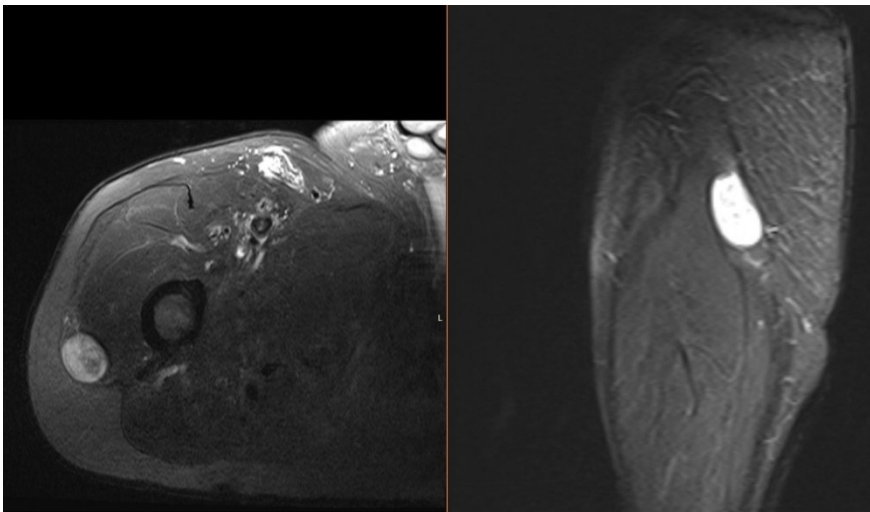
Picture 1: The patient's thoracic CT scan revealed a slow-growing rib tumor.

Despite the growth of the lesion, the diagnosis was delayed due to imaging errors. The lesion was misinterpreted at various stages, leading to progression of the disease without proper identification. After the lesion's continued enlargement and the onset of local invasion into adjacent bone and muscle tissue, a biopsy was finally performed. The biopsy revealed the presence of an atypical carcinoid tumor with local invasion into bone and muscle.

Further investigation, including MRI, revealed an additional tumor in the right leg, which was diagnosed as a schwannoma via a

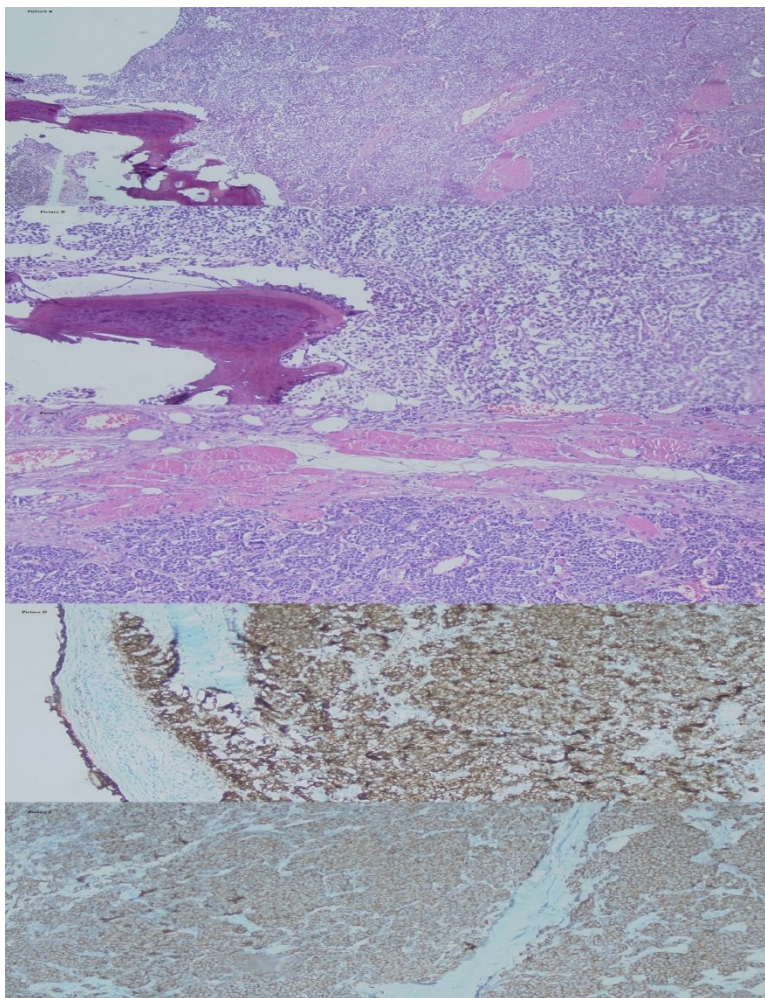
trucut biopsy. The diagnosis of schwannoma was subsequently confirmed by three different pathology departments.

Surgical excision is planned by the orthopedic surgeon. Comparing the current MRI with images from 10 months ago, a lesion near the proximal right vastus lateralis is seen. On T1-weighted imaging, it appears hypointense, and on fluid-sensitive sequences, it is heterogeneously hyperintense. After contrast, the lesion shows peripheral and septal enhancement with well-defined borders, measuring 26 x 19 x 37 mm, adjacent to the right iliotibial band. On T2-weighted imaging, it is hyperintense with similar enhancement patterns. The lesion's size and characteristics remain unchanged, consistent with the previous diagnosis of schwannoma. Picture 2.,



Picture 2 MRI of the right leg : After contrast, the lesion shows peripheral and septal enhancement with well-defined borders, measuring 26 x 19 x 37 mm, adjacent to the right iliotibial band.

In January 2024, the patient underwent surgical resection of the 9th and 10th ribs, with reconstruction performed using Prolene mesh. The final pathology report confirmed the diagnosis of an atypical carcinoid tumor.(Picture 3 A,B,D,C,E)



Picture 3 A,B,D,C,E Figures A and B: Tumoral development is observed, consisting of uniform cells with small nuclei, eosinophilic, narrow cytoplasm, and granular chromatin,

infiltrating the surrounding bone tissue in a solid pattern (H&E, x100 and H&E, x200). Figure C: The tumor shows infiltration into the surrounding muscle tissue (H&E, x200). Figure D: The tumor demonstrates diffuse immunoreactivity for the neuroendocrine marker CD56 (x200). Figure E: Positive immunoreactivity is observed with another marker, Chromogranin (x200).

After surgery, the patient received adjuvant chemotherapy and radiotherapy. Nine months later, the patient was successfully treated for pulmonary thromboembolism (PTE), a known complication in patients with carcinoid tumors.

A follow-up 68Ga-DOTA-TATE PET/CT scan, performed 11 months post-surgery, showed no clear focus of recurrence or metastasis. Although there was some increased uptake in the area of the previous lesion, the findings did not suggest definitive recurrence, and no new lesions were identified.

Additionally, the patient's prior cholecystectomy specimen, which had been re-evaluated by the pathologist, showed no evidence of carcinoid cells. This re-evaluation helped confirm that the gallbladder was not a source of the primary carcinoid tumor, ruling out the possibility of a gallbladder-originated neuroendocrine tumor.

DISCUSSION

Carcinoid tumors, though relatively uncommon, present a significant clinical challenge due to their potential for metastasis and the distinct biological behavior they exhibit. These neuroendocrine tumors can arise in various organs, but the most frequent sites are the gastrointestinal (GI) tract (particularly the small intestine, appendix, and colon), followed by the lungs. Other, less common locations include the pancreas, liver, and ovaries. Primary bone localization of carcinoid tumors is extremely rare. Their biological behavior and

risk of metastasis can vary depending on their origin, degree of differentiation, and histological features.(Moddlin ,2005, 92–101, Hori, 2012, 1105-1108).

Carcinoid tumors are typically classified as either "typical" or "atypical", based on their differentiation and mitotic activity. "Typical" carcinoids are well-differentiated, showing the classical histological architecture of trabecular, insular, or ribbon-like cell clusters with minimal pleomorphism and low mitotic rates. In contrast, "atypical" carcinoids are more aggressive, with higher mitotic activity and a greater potential for metastasis. (Norheim, 1987, 120).The classification by embryological origin-foregut, midgut, and hindgut-remains useful but is less commonly utilized due to its limited clinical relevance. It does, however, provide insight into the characteristic features of carcinoids originating from each region, such as hormonal secretion patterns and propensity for metastasis.(Gade, 2020, 1;Moddlin 2003, 934-959).

One of the key aspects of carcinoid tumors is their metastatic behavior. The liver is the most frequent site for metastases, followed by the lungs and lymph nodes. Skeletal metastases are uncommon, but when they do occur, the spine (especially the thoracic vertebrae), ribs, and pelvis are the most likely sites. (Moddlin ,2005, 92–101, Hori, 2012, 1105-1108).In the present case, the primary carcinoid tumor was located in the rib, a rare occurrence, making this case an unusual presentation for a carcinoid tumor.

The association of other malignancies with carcinoid tumors has been well documented, with studies indicating that 22.4%-44.5% of patients with carcinoid tumors also present with coexisting malignancies. In particular, gastrointestinal carcinoids are more

likely to coexist with other neoplasms, including adenocarcinomas of the colon, rectum, and small bowel. This phenomenon is thought to result from the proliferative peptides secreted by carcinoid tumors, which may promote the development or growth of secondary tumors. (Moddlin, 2005, 92–101)

The coexistence of another tumor, such as a schwannoma, in this case, further complicates the diagnostic landscape. Schwannomas are benign tumors of the peripheral nervous system. Their occurrence in the lower limbs is extremely rare, accounting for only 1% of schwannoma cases. Furthermore, the presence of a schwannoma alongside a carcinoid tumor has not been reported before. (Kutalia, 2024, 1-4; Quang, 2023: 1-6) The pathophysiology of such concurrent tumors is not well understood but may reflect independent tumorigenesis in separate cell types or perhaps a shared underlying genetic or environmental factor influencing both tumors.

One important aspect of this case was the re-evaluation of the patient's previous cholecystectomy specimen. The gallbladder had been removed a year prior, and upon review, the pathologist confirmed that no carcinoid cells were present. This was an important finding because it helped rule out the possibility that the gallbladder might have been the source of the primary carcinoid tumor. Carcinoid tumors in the gallbladder are extremely rare, but their possibility could not be dismissed without careful histological examination. This emphasizes the importance of re-evaluating past medical records and specimens when new, unexpected diagnoses arise.

Advanced imaging modalities are crucial in diagnosing carcinoid tumors, especially when they arise in atypical sites. While

CT scans, MRI, and PET/CT scans are often used to visualize these tumors, octreotide scintigraphy (which uses radiolabeled somatostatin analogs) and other specialized imaging techniques like somatostatin receptor imaging can help detect carcinoid tumors that are not always visible on standard imaging. (Scarsbrook, 2007,455; Hori, 2012, 1108) In this case, the initial CT scan missed the diagnosis, but a biopsy ultimately provided a definitive diagnosis. This underlines the necessity for a multi-modal approach when investigating suspected carcinoid tumors.

Treatment for carcinoid tumors primarily involves surgical resection, particularly when the tumor is localized and there is no evidence of widespread metastasis. In this patient's case, rib resection followed by reconstruction was successful. Adjuvant therapies like chemotherapy and radiotherapy are used based on the tumor's histological features, including its aggressiveness and potential for metastasis. This patient received both chemotherapy and radiotherapy, reflecting the atypical nature of the tumor and its potential for recurrence. Despite these treatments, the follow-up PET/CT scan showed no evidence of recurrence, which is a positive outcome.

Conclusion:

This case of an atypical carcinoid tumor located in the rib, coexisting with a schwannoma in the leg, is an extremely rare presentation of neuroendocrine tumors. The unusual combination of these two tumors highlights the importance of a comprehensive diagnostic approach, including advanced imaging and careful histopathological evaluation. The re-evaluation of the gallbladder specimen helped exclude it as the source of the primary carcinoid

tumor, a crucial step in narrowing down the tumor's origin. Surgical resection remains the cornerstone of treatment for localized carcinoid tumors, and adjuvant therapies can be beneficial in high-risk cases. Regular follow-up with imaging is essential to detect any recurrence or metastasis, although in this case, the prognosis appears favorable due to the absence of new findings on follow-up imaging. Awareness of rare presentations of carcinoid tumors is important for clinicians to ensure prompt and accurate diagnosis, leading to better outcomes for patients.

REFERENCES

Gade A K, Olariu E, Douthit N T (2020, March) Carcinoid Syndrome: A Review. Cureus 12(3): e7186. DOI 10.7759/cureus.7186

Hori T, Yasuda T, Suzuki K, Kanamori M, Kimura T. (2012) Skeletal metastasis of carcinoid tumors: Two case reports and review of the literature. Oncology Letters, 3: 1105-1108,

İncekara F, Findik G, Aydoğdu K, FTanrıkulu FB. (2019). A Rare Rib Lesion due to Atypical Carcinoid Tumor: A Case Report. Turk Thorac J, 20(s1): 394. DOI: 10.5152/TurkThoracJ.2019.299

Kutalia N, Bolkvadze M, Mehmet N Erdem.MN, Schwannoma of the Lower Limb: A Case Report . Cureus. 2024 Aug 11;16(8):e66616. doi: 10.7759/cureus.66616

Modlin, IM., Lye, KD, Kidd MA (2003). A 5-Decade Analysis of 13,715 Carcinoid Tumors. Cancer, 97(4): 934-959

Modlin IM , Shapiro MD, Kidd M, (2005) An Analysis of Rare Carcinoid Tumors: Clarifying These Clinical Conundrums. World J. Surg., 29:92–101 DOI: 10.1007/s00268-004-7443-z

Norheim, K Oberg, E Theodorsson-Norheim, P G Lindgren, G Lundqvist, A Magnusson, L Wide, E Wilander (1987, Aug)Ann Surg. Malignant carcinoid tumors. An analysis of 103 patients with regard to tumor localization, hormone production, and survival. 206(2):115-25. doi: 10.1097/00000658-198708000-00001.

Scarsbrook A.F., Ganeshan A, Statham J, Thakker RV, Weaver A, et al. (2007 Mar-Apr) Radiographics. Anatomic and

functional imaging of metastatic carcinoid tumors, 27(2):455-77.
doi: 10.1148/rg.272065058.DOI: 10.1148/rg.272065058

Quang V.P , Quoc HH , Nguyen B, Quang C.N, Chi H.N.,
Nguyen N.(2023) Giant schwannoma on the lower leg: a case report
and review of the literature. Int J Surg Case Rep, 109:108468. doi:
10.1016/j.ijscr.2023.108468

Zuetenhorst JM, Babs G. B. (2005). Metastatic Carcinoid
Tumors: A Clinical Review. The Oncologist;10:123-131

